ARTICLE

# Study of Cadmium-Doped Zinc Oxide Nanocrystals with Composition and Size Dependent Band Gaps

Hai-xiao Zhang, Yue-tao Yang*, Xiao-jun Liu

*Key Laboratory of Modern Acoustics, Ministry of Education, Institute of Acoustics, Nanjing University, Nanjing 210093, China*

(Dated: Received on September 28, 2017; Accepted on January 9, 2018)

Cadmium-doped zinc oxide nanocrystals in the quantum confinement region have been firstly synthesized by a fast and facile sonochemical method. The alloyed structure of the nanocrystals is confirmed by X-ray diffraction, transmission electron microscopy, and infrared analysis. With the increase of cadmium to zinc molar ratio from 0 to 2.0, the crystallite sizes of the samples decrease from 5.1 nm to 2.6 nm, and the band gaps of the samples show a red shift then a blue shift, and a red shift again. The variations of band gaps of the samples can be interpreted by the crystallite size and the composition. It is found that both the non-thermal equilibrium environment established in the sonochemical reaction and the coordination ability of triethylene glycol solvent play crucial roles in the current preparation.

**Key words:** Alloyed nanocrystal, Structure, Spectroscopy, Sonochemistry

## I. INTRODUCTION

Since the beginning of the twentieth century, the band gap engineering of semiconductor nanomaterials has given rise to intriguing science [1−6]. Generally, tuning the size of nanomaterials is one way of adjusting the band gap energy [2]. Another means of tailoring the semiconductor band gap is by changing the constituent stoichiometries of nanomaterials [3−6]. Zinc oxide nanomaterials are of great importance because of their excellent electronic, optical and luminescent properties [7, 8]. However, the construction of zinc oxide nanomaterials with composition-dependent band gap in the quantum confinement region remains a challenge for scientists.

Cadmium-zinc oxide alloys have attracted increasing attention for using as light emitting sources, transparent solar cells, biomedical imaging materials, and water splitting reagents [9−12]. The wurtzite phase of zinc oxide, however, is not compatible with the rock-salt phase of cadmium oxide [13]. There have been a few reports on the synthesis of cadmium-doped zinc oxide nanomaterials via the sol-gel method, but the maximum concentration of cadmium is usually below 10 mol% [14, 15]. It thus suggests that preparation cadmium-doped zinc oxide nanomaterials with a broad composition range should rely on the non-thermal equilibrium growth condition [16].

The sonochemical method has become a powerful tool to prepare many kinds of nanomaterials [17]. The extreme but transient local conditions caused by acoustic cavitation can establish a highly non-thermal equilibrium environment [17−19]. Phuruangrat *et al.* reported sonochemical synthesis of cadmium-doped zinc oxide nanocrystals with an average crystallite size of 45 nm [20], however, no quantum confinement effect can be found for these nanocrystals because of the large crystallite size. Recently, lanthanide and cadmium ions doped zinc oxide nanocrystals have been synthesized via the sonochemical method in our laboratory [21−23]. It was found that cadmium content up to 40% can be achieved, but the crystallite sizes of the samples are too large to show the quantum confinement effect [23]. To the best of our knowledge, cadmium-doped zinc oxide nanocrystals in the quantum confinement region have not been reported to date. Cadmium-alloyed zinc oxide nanocrystals possess additional properties that are composition-dependent aside from the properties that emerge due to quantum confinement effects. The study of these materials is not only of fundamental interest, because these materials are also important and useful to construct appropriate ZnO-related heterostructures or quantum well structures, which are the key elements in ZnO-based light emitters and detectors [24, 25]. In this work, cadmium-doped zinc oxide nanocrystals in the quantum confinement region have been synthesized via a sonochemical method for the first time. For the samples with cadmium to zinc molar ratio from 0 to 2.0, the homogenous structure is confirmed by the X-ray diffraction, transmission electron microscopy and infrared analysis. These nanocrystals exhibit size and composition-dependent band gaps. Moreover, a plausible formation mechanism has been proposed for the

*Author to whom correspondence should be addressed. E-mail: yyang@nju.edu.cn, FAX: +86-25-83315557.

 

current sonochemical preparation.

## II. EXPERIMENTS

### A. Synthesis of cadmium-doped zinc oxide nanocrystals

Zinc acetate dihydrate (0.002 mol) and lithium hydroxide monohydrate (0.003 mol) were dissolved by 40 mL triethylene glycol in a 100-mL glass vial. Cadmium acetate dihydrate was then added to the above solution according to the molar ratio of Cd to Zn (denoted as $A$). The value of $A$ was 0, 0.15, 0.30, 0.60, 1.0 or 2.0, respectively. Each solution was sonicated continuously at room temperature in ambient air for 2 min, and the final temperature of the solution was (96±10) °C. The sonication was operated with a VCX-750 ultrasonic generator at an electronic power of 500 W and an ultrasonic frequency of 20 kHz. The solution was cooled in an ice-water bath. Ethyl acetate was added to the above solution to precipitate the nanocrystals, and the precipitate was redispersed in absolute ethanol. The precipitation-redispersion treatment was repeated for several times to purify the products thoroughly. The obtained colloids were used for further characterizations. Parallel experiments were performed with the same procedure described above, except for changes in solvents and the ultrasound treatment.

### B. Materials and physical techniques

All reagents and solvents for the syntheses and analyses were of analytical reagent grade (Sinopharm Chemical Reagent Co., Ltd., Shanghai, China). Transmission electron microscopy (TEM) images were recorded on a Jeol JEM-200CX microscopy. Absorption spectra of the colloidal nanocrystals in ethanol were measured at room temperature on a Shimadzu UV240 spectrophotometer. The ethanol solutions of the samples were then vaporized and dried at 100 °C. The obtained powders were used for X-ray diffraction (XRD) and infrared analysis. XRD experiments were performed on a Thermo Electron Corporation ARLX'TRA-48 X-ray diffractometer using Cu K$\alpha$ radiation. Infrared (IR) spectra were measured on a Nicolet Nexus 870 infrared spectrometer. The actual cadmium to zinc molar ratios of the samples were determined on a Shimadzu ICPS-7500 inductively coupled plasma mass spectrometer.

## III. RESULTS AND DISCUSSION

### A. Structural study of cadmium-doped zinc oxide nanocrystals

TEM imagines of Cd-ZnO nanocrystals are shown in FIG. 1. It is found that the samples are uniform spherical nanocrystals with narrow size distributions. High resolution TEM images show that the samples have a wurtzite structure. The crystallite sizes of the samples are inversely proportional to $Cd^{2+}$ content, ranging from 5 nm to 2.5 nm approximately.

XRD spectra of the samples are shown in FIG. 2. It can be found that all the samples have a wurtzite structure. The XRD patterns in FIG. 1 correspond to (100), (002), (101), (102), (110), (103), and (112) reflections of a wurtzite structure (JCPDS Card 36-1451). The results demonstrate there is no phase separation or separated nucleation of CdO or ZnO nanocrystals. The alloyed structure is supported by the XRD spectra of the nanocrystals, in which the diffraction peaks systematically shift to small angles with the increase of $Cd^{2+}$ content. Although the lattice volumes of nanocrystals may change with reducing the crystallite size because of surface stresses, oxygen vacancies or broken coordination, the lattice spacing has been found to be stationary for pure ZnO colloids with diameters ranging from 2 nm to 5 nm [26]. The shifts of XRD peaks with the increase of $Cd^{2+}$ content are dominantly due to the size difference between $Cd^{2+}$ (0.97 Å) and $Zn^{2+}$ (0.74 Å) ions [27].

In the insert of FIG. 2, the lattice parameter $c$ measured from XRD patterns of the nanocrystals exhibits a linear relationship with the molar fraction of $Cd^{2+}$. The variation of lattice parameter $c$ from 5.21 Å to 5.44 Å is in accordance with Vegard's law, and is consistent with the result of Cd-ZnO alloys [13, 28]. This further confirms the formation of homogeneous nanocrystals. Swafford *et al.* characterized the uniformity of particles with the periodic removal of aliquots of the growing nanocrystals, and analyzed the aliquots to determine composition [29]. The method is not suitable here because of the very fast synthesis processes. Crystallite sizes of the samples have been determined using Scherrer's equation, *i.e.*, $D=0.9\lambda/B\cos\theta$, where $D$ is the average crystallite size, $\lambda$ is the wavelength of 0.15418 nm from Cu K$\alpha$ radiation, $B$ is the full-width at half-maximum of the diffraction peak and $\theta$ is the Bragg angle [30]. The crystallite sizes are 5.1, 4.1, 3.8, 3.2, 2.7, and 2.6 nm, respectively, for the samples with $A$=0, 0.15, 0.30, 0.60, 1.0, and 2.0. The diffraction peaks of the samples are broad and weak because of the small crystallite sizes and the decrease of crystallinity. Actual Cd/Zn molar ratios for the samples have been measured by inductively coupled plasma mass spectrometer. For the samples with $A$=0, 0.15, 0.30, 0.60, 1.0, and 2.0, the measured values are 0, 0.15, 0.29, 0.58, 0.97, and 1.9, respectively.

IR spectra of the samples are shown in FIG. 3. One broad IR absorption band appears around 464 $cm^{-1}$ for pure ZnO sample, which is consistent with the calculated and experimental results for spherical ZnO particles [31, 32]. The maximum of Zn−O IR band shows a systematical red shift from 464 $cm^{-1}$ at $A$=0 to 449 $cm^{-1}$ at $A$=2 in FIG. 3(b). It indicates a continuous lattice expansion due to the substitution of $Cd^{2+}$ in

DOI:10.1063/1674-0068/31/cjcp1708181 

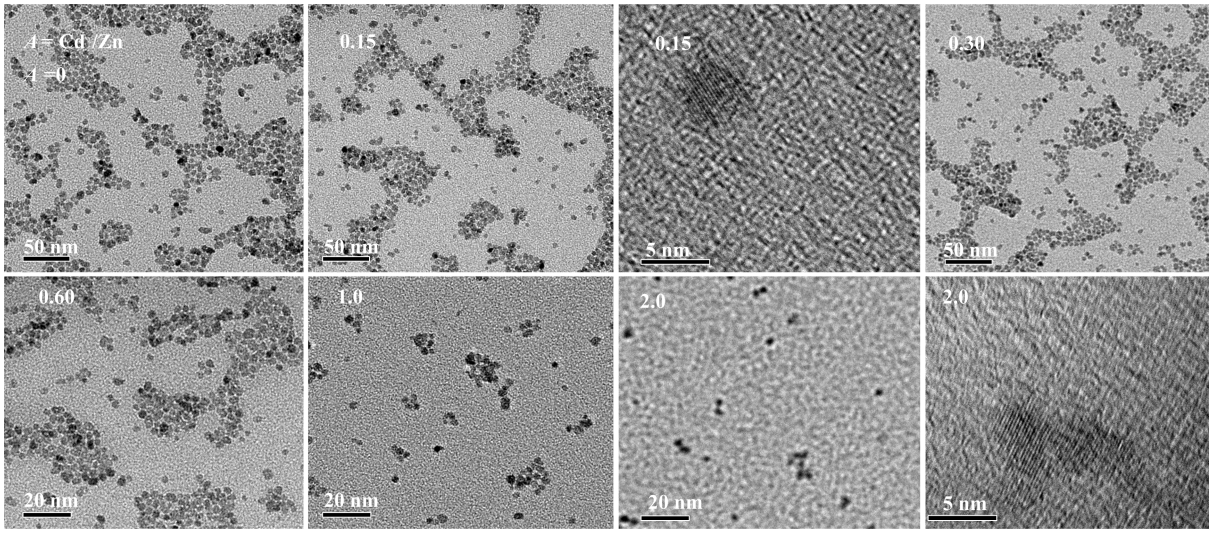


FIG. 1 TEM images of cadmium-doped zinc oxide nanocrystals with different cadmium to zinc molar ratio $A$.

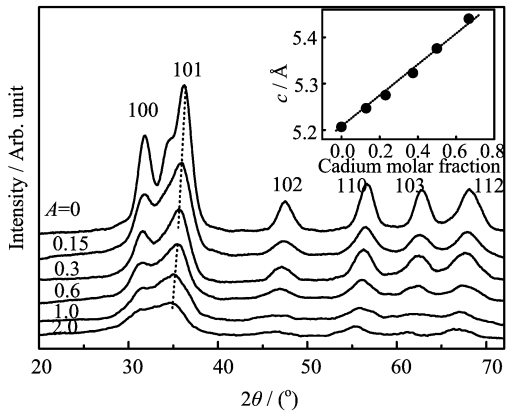


FIG. 2 XRD patterns of cadmium-doped zinc oxide nanocrystals with different cadmium to zinc molar ratio $A$. Relationship of lattice parameter $c$ as a function of cadmium molar fraction (inserted figure).

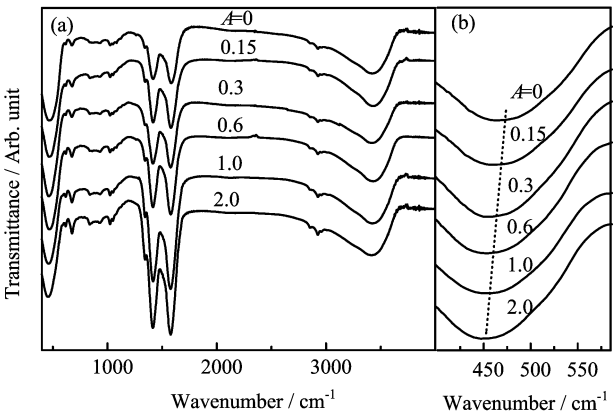


FIG. 3 Infrared spectra of cadmium-doped zinc oxide nanocrystals with different cadmium to zinc molar ratio $A$.

ZnO lattice. IR bands in the region of 1700−600 $cm^{-1}$ correspond to C=O, C−O, and C−H vibrations of the acetate group. No absorption bands of zinc hydroxide or cadmium hydroxide can be found in the IR spectra. It suggests that no phase segregation or secondary phase has formed for the samples.

### B. Band gap study of cadmium-doped zinc oxide nanocrystals

Absorption spectra of the samples are shown in FIG. 4. The band gap $E_g$ of the samples can be obtained with Tauc's equation $(\alpha h\nu)=C(h\nu-E_g)^n$ [33], where $\alpha$ is the absorption coefficient, $C$ is the constant and $h\nu$ is the photon energy. For crystalline semiconductors, the exponent $n$ in Tauc's equation can take the value 1/2, 3/2, or 2 when the transitions are direct allowed, direct forbidden or indirect allowed, respectively. The band gap $E_g$ can be obtained from the extrapolation of the straight-line portion of the $(\alpha h\nu)^{1/n}$ *vs.* $h\nu$ plot to $h\nu$=0. It is observed that for all the samples, the best straight line is obtained for $n$=1/2, which is expected for direct allowed transition of Cd-ZnO alloys [16, 34]. The dashed curves in FIG. 4 show the best fitted results.

The behavior of alloys is characterized by Vegard's Law [28], which states that, while lattice constant changes linearly with composition, other physical properties such as band gap often vary nonlinearly. The nonlinearity is usually deemed to come from three sources, namely, the volume deformation, the chemical electronegativity difference and the internal structural relaxation [35]. Moreover, in the case of nanocrystals of any composition, quantum confinement also induces a size dependence [36]. Thus the variation of band gap

DOI:10.1063/1674-0068/31/cjcp1708181 

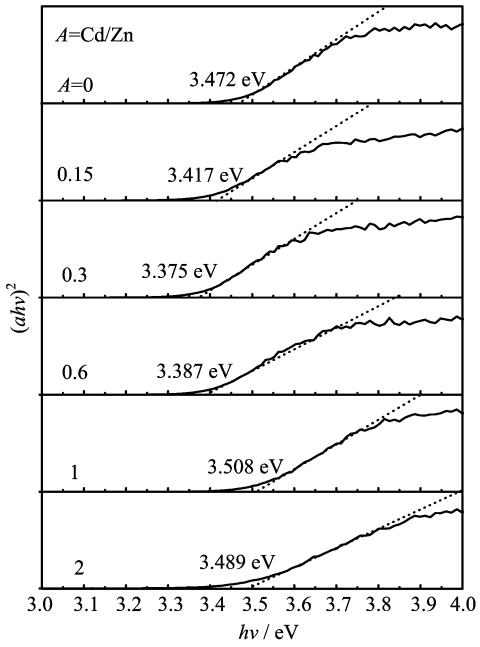


FIG. 4 Absorption spectra of cadmium-doped zinc oxide nanocrystals with different cadmium to zinc molar ratio $A$.

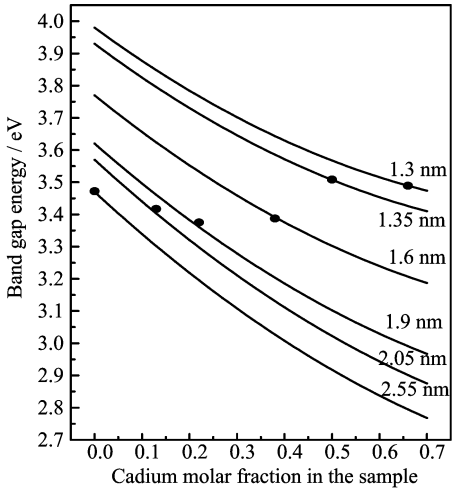


FIG. 5 Crystallite radius and composition-dependent band gaps of cadmium-doped zinc oxide nanocrystals.

energies of the samples can be attributed to both the composition and quantum confinement effect. The experimental data were fitted by the expression:

$$E_{\rm g}^{\rm Cd\text{-}ZnO}(x) = E_{\rm g}^{\rm CdO}x + E_{\rm g}^{\rm ZnO}(1-x) - bx(1-x) \quad (1)$$

where $x$ is the molar fraction of $Cd^{2+}$ in Cd-ZnO nanocrystals, and $b$ is the bowing parameter which describes the nonlinearity. For the samples of any composition, quantum confinement also introduces a size dependence [36]:

$$E_{\rm g}(R) = E_{\rm g}^{\rm bulk} + \frac{h^2}{8\mu R^2} - \frac{1.8e^2}{4\pi\varepsilon\varepsilon_0 R} \quad (2)$$

where $E_{\rm g}(R)$ is the band gap of the nanocrystals, $R$ is the radius of the crystal, $\mu$ is the effective mass of the exciton, $h$ is Plank's constant, $\varepsilon$ is the relative permittivity, $\varepsilon_0$ is the permittivity of free space and $e$ is the charge on the electron. Substituting Eq.(2) into Eq.(1), the dependence of band gap on crystallite size and composition can be derived as below [29]:

$$E_{\rm g}(x,R) = \left[E_{\rm g}^{\rm bulk\ CdO} + \frac{h^2}{8\mu_{\rm CdO}R^2} - \frac{1.8e^2}{4\pi\varepsilon\varepsilon_0 R}\right]x + \left[E_{\rm g}^{\rm bulk\ ZnO} + \frac{h^2}{8\mu_{\rm ZnO}R^2} - \frac{1.8e^2}{4\pi\varepsilon\varepsilon_0 R}\right]\cdot (1-x) - b(R)x(1-x) \quad (3)$$

In Eq.(3), the bowing parameter $b$ is treated as a function of the nanocrystal radius. With the values of $E_{\rm g}{}^{\rm bulk}$ and $\mu$ of CdO and ZnO [37], the band gaps have been calculated based on Eq.(3). The results are shown in FIG. 5, where the solid lines are theoretical values at certain radius of Cd-ZnO nanocrystals and the dots are the experimental results.

It can be found in FIG. 5 that the samples are in the quantum confinement region. The variation of the band gap can be elucidated well based on the crystallite size and the composition, yielding a constant bowing parameter of 0.61 eV for the samples. With the increase of $A$ from 0 to 0.3, the band gap decreases from 3.472 eV to 3.375 eV. At low doping level, the variation of band gaps mainly reflects the trend of the composition effect because the crystallite sizes of the samples are relatively large. With the increase of $A$ from 0.3 to 1.0, the band gap increases from 3.375 eV to 3.508 eV. This is because that the crystallite sizes of the samples are small and the quantum confinement effect plays a main role in the band gap energy. With further increase of $A$ from 1.0 to 2.0, the band gap decreases again. As the crystallite sizes of the samples with $A$=1.0 and 2.0 are quite similar, the remarkable increase of $Cd^{2+}$ content in the sample results in the decrease of the band gap energy.

For Cd-ZnO alloys, the reported values of bowing parameter deviate between different studies. The value of bowing parameter in this work is less than the values of 1.26 and 0.95 eV [38, 39], but is greater than the values of 0.45 and 0.54 eV [27, 40]. This is presumably due to different crystal structures and analytical methods. It might have been expected that the small change in lattice spacing, the surface effect and surrounding environment of nanocrystals can significantly impact the bowing parameter. The result in this work indicates that those effects mentioned above are not strong enough to impact the bowing behavior of the samples. The bowing parameter is in fact not sensitive to radius, in agreement with previous works on $Zn_xCd_{1-x}Se$ and $CdS_xSe_{1-x}$ [29, 41].

DOI:10.1063/1674-0068/31/cjcp1708181 

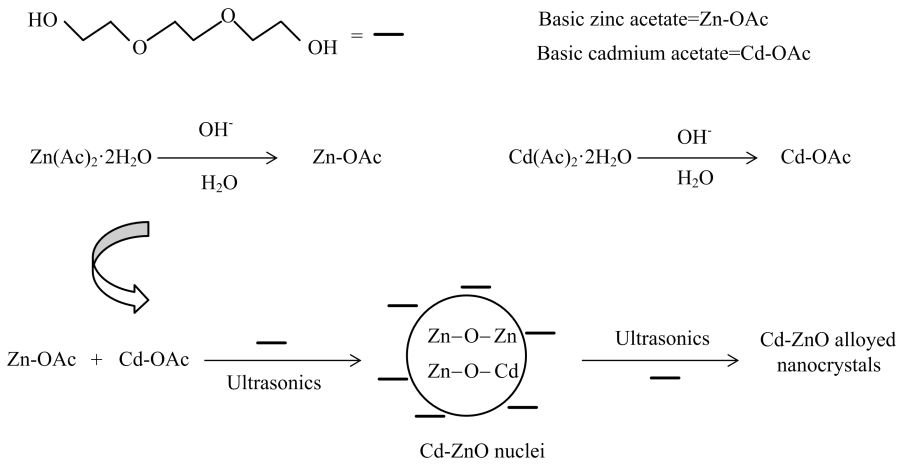


FIG. 6 Schematic illustration of the formation process for cadmium-doped zinc oxide nanocrystals in triethylene glycol upon ultrasonic irradiation.

### C. Sonochemical formation mechanism of the nanoparticles

In order to investigate the effect of both solvents and the irradiation of ultrasound on the preparation of the products, parallel experiments were carried out. Anhydrous ethanol or an ionic liquid, 1-butyl-3-methylimidazolium tetrafluoroborate has been chosen to substitute for triethylene glycol. Anhydrous ethanol is the most commonly used solvent in sol-gel preparation of ZnO nanocrystals. The ionic liquid has a negligible vapour pressure and a high decomposition point (300 °C), which is similar to triethylene glycol with a high boiling point (287 °C). Experimental results show that only mixtures of CdO and ZnO can be obtained in the two parallel reactions. Moreover, the parallel experiment without ultrasound treatment shows that no products can be obtained. These results demonstrate that both the ultrasonic irradiation and triethylene glycol play crucial roles in the present preparation.

Based on the above experimental results, a plausible preparation mechanism of Cd-ZnO nanocrystals is proposed in FIG. 6. In the presence of $LiOHH_2O$, metal acetates transfer to basic acetate precursors, denoting as Zn-OAc and Cd-OAc [42]. Upon ultrasonic irradiation, highly non-thermal equilibrium environment can be established in triethylene glycol solution. This favors homogenous nucleation processes through hydrolysis and condensation reactions of the basic acetate precursors. For the wurtzite crystal, the top surface (0001) is $Zn^{2+}$ or $Cd^{2+}$ terminated and the bottom surface $(000\bar{1})$ is $O^{2-}$ terminated. Additionally, the wurtzite crystal has other $O^{2-}$ terminated surfaces. The wurtzite crystal needs the smallest active energy to grow along the (0001) direction [25]. However, triethylene glycol can strongly coordinate to metal ions on this surface, prohibiting the anisotropic growth of the nanocrystals. Although triethylene glycol can also form hydrogen bonds with terminated $O^{2-}$ ions, some active sites can be produced randomly on the surfaces of ZnO nuclei due to the enhanced mobility triggered by the ultrasonic irradiation. This reaction environment results in the isotropic growth of spherical nanocrystals.

With the increase of $Cd^{2+}$ content, the crystallinity of the samples decreases remarkably, which will prevent the continuous growth of wurtzite crystals. Meanwhile, triethylene glycol can effectively stabilize the small crystals by coordination bonds or hydrogen bonds with terminated metal ions or $O^{2-}$ ions on the surfaces of the crystals, resulting in the decrease of the crystallite size.

## IV. CONCLUSION

Cadmium-doped zinc oxide nanocrystals have been firstly synthesized in the quantum confinement region. The band gaps of the samples can be interpreted well based on both the quantum confinement effect and the constituent stoichiometry. The formation of the nanocrystals mainly arises from the non-thermal equilibrium environment established in sonochemical reaction and the coordination ability of triethylene glycol. The fast, facile and green sonochemical approach is promising to prepare other nanomaterials with non-equilibrium structures.

## V. ACKNOWLEDGMENTS

This work was supported by the National Basic Research Program of China (No.2012CB921504) and the National Natural Science Foundation of China (No.11074127).

[1] M. Schwarze, W. Tress, B. Beyer, F. Gao, R. Scholz, C. Poelking, K. Ortstein, A. A. Gunther, D. Kasemann, D. Andrienko, and K. Leo, Science **352**, 1446 (2016).

DOI:10.1063/1674-0068/31/cjcp1708181 

[2] A. M. Smith and S. Nie, Acc. Chem. Res. **43**, 190 (2009).
[3] M. D. Regulacio and M. Y. Han, Acc. Chem. Res. **43**, 621(2010).
[4] H. Wei, S. Z. Chen, X. L. Ren, B. J. Qian, Y. J Su, Z. Yang, and Y. F. Zhang, CrystEngComm **14**, 7408 (2012).
[5] H. Wei, Y. J. Su, Z. Y. Han, T. T. Li, X. L. Ren, Z. Yang, L. M. Wei, F. S. Cong, and Y. F. Zhang, Nanotechnology **24**, 235706 (2013).
[6] H. Wei, X. L. Ren, Z. Y. Han, T. T. Li, Y. J. Su, L. M. Wei, F. S. Cong, and Y. F. Zhang, Mater. Lett. **102**, 94 (2013).
[7] A. B. Djurisic and Y. H. Leung, Small **2**, 944 (2006).
[8] B. Wen, C. Q. Liu, N. Wang, H. L. Wang, S. M. Liu, W. Y. Ding, W. D. Fei, and W. P. Chai, Chin. J. Chem. Phys. **29**, 229 (2016).
[9] N. Kumar and A. Srivastava, J. Alloys Compd. **706**, 438 (2017).
[10] J. Zhang, S. Q. Zhao, K. Zhang, and J. Q. Zhou, Chemosphere **95**, 105 (2014).
[11] M. A. Mansoor, M. A. Ehsan, V. McKee, N. M. Huang, M. Ebadi, Z. Arifin, W. Z. Basiruna, and M. Mazhar, J. Mater. Chem. **17**, 5284 (2013).
[12] S. Chu and G. Wang, Mater. Lett. **85**, 149 (2102).
[13] J. Ishihara, A. Nakamura, S. Shigemori, T. Aoki, and J. Temmyo, Appl. Phys. Lett. **89**, 091914 (2006).
[14] A. A. Jacob, L. Balakrishnan, S. R. Meher, K. Shambavi, and Z. C. Alex, J. Alloys Compd. **695**, 3753 (2017).
[15] B. Khodadadi, M. Bordbar, and A. Y. Faal, J. Sol-Gel Sci. Tech. **77**, 521 (2016).
[16] D. M. Detert, S. H. M. Lim, K. Tom, A. V. Luce, A. Anders, O. D. Dubon, K. M. Yu, and W. Walukiewicz, Appl. Phys. Lett. **102**, 232103 (2013).
[17] J. J. Hinman and K. S. Suslick, Top. Curr. Chem. **375**, 12 (2017).
[18] J. H. Bang and K. S. Suslick, Adv. Mater. **22**, 1039 (2010).
[19] D. G. Shchukin and H. Mohwald, Phys. Chem. Chem. Phys. **8**, 3496 (2006).
[20] A. Phuruangrat, S. Mad-ahin, O. Yayapao, S. Thongtem, and T. Thongtem, Res. Chem. Intermed. **41**, 9757 (2015).
[21] H. X. Zhang, B. Gao, Y. T. Yang, and X. J. Liu, Int. J. Thermophys. **36**, 1336 (2015).
[22] B. Gao, Y. T. Yang, H. Yang, S. Y. Zhang, and X. J. Liu, Sci. China-Phys. Mech. Astron. **56**, 1280 (2013).
[23] Y. Wang, Y. T. Yang, X. G. Zhang, X. J. Liu, and A. Nakamura, CrystEngComm **14**, 240 (2012).
[24] T. Noorunisha, V. S. Nagarethinam, M. Suganya, D. Praba, S. Ilangovan, K. Usharani, and A. R. Balu, Optik **127**, 2822 (2106).
[25] U. Ozgur, Y. I. Alivov, C. Liu, A. Teke, M. A. Reshchikov, S. Dogan, V. Avrutin, S. J. Cho, and H. Morkoc, J. Appl. Phys. **98**, 041301 (2005).
[26] A. Wood, M. Giersig, M. Hilgendorff, A. V. Campos, L. M. Marzan, and P. Mulvaney, Aust. J. Chem. **56**, 1051 (2003).
[27] O. Vigil, L. Vaillant, F. Cruz, G. Santana, A. M. Acevedo, and G. C. Puente, Thin Solid Films **361**, 53 (2000).
[28] L. Vegard, Z. Phys. **5**, 17 (1921).
[29] L. A. Swafford, L. A. Weigand, M. J. Bowers, J. R. McBride, J. L. Rapaport, T. L. Watt, S. K. Dixit, L. C. Feldman, and S. J. Rosenthal, J. Am. Chem. Soc. **128**, 12299 (2006).
[30] A. Burns, G. Hayes, W. Lia, J. Hirvonen, J. D. Demaree, and S. I. Shah, Mater. Sci. Eng. B **111**, 150 (2004).
[31] H. Kleinwechter, C. Janzen, J. Knipping, H. Wiggers, and P. Roth, J. Mater. Sci. **37**, 4349 (2002).
[32] M. A. Verges, A. Mifsud, and C. J. Serna, J. Chem. Soc. Faraday Trans. **86**, 959 (1990).
[33] J. I. Pankove, *Optical Processes in Semiconductors*, New York: Englewood Cliffs, 34 (1971).
[34] X. F. Fan, H. D. Sun, Z. X. Shen, J. L. Kuo, and Y. M. Lu, J. Phys.: Condens. Matter **20**, 235221 (2008).
[35] J. E. Bernard and A. Zunger, Phys. Rev. B **36**, 3199 (1987).
[36] K. F. Lin, H. M. Cheng, H. C. Hsu, L. J. Lin, and W. F. Hsieh, Chem. Phys. Lett. **409**, 208 (2005).
[37] B. J. Zheng, J. S. Lian, L. Zhao, and Q. Jiang, Appl. Surf. Sci. **257**, 5657 (2011).
[38] D. W. Ma, Z. Z. Ye, and Y. S. Yang, Appl. Phys. B **82**, 85 (2006).
[39] X. J. Wang, I. A. Buyanova, W. M. Chen, M. Izadifard, S. Rawal, D. P. Norton, S. J. Pearton, A. Osinsky, J. W. Dong, and A. Dabiran, Appl. Phys. Lett. **89**, 151909 (2006).
[40] I. A. Buyanova, X. J. Wang, W. M. Chen, M. Izadifard, D. P. Norton, S. J. Peartonc, A. Osinsky, J. W. Dong, and A. Dabiran, ECS Trans. **3**, 391 (2006).
[41] X. H. Zhong, M. Y. Han, Z. L. Dong, T. J. White, and W. Knoll, J. Am. Chem. Soc. **125**, 8589 (2003).
[42] E. A. Meulenkamp, J. Phys. Chem. B **102**, 5566 (1998).

DOI:10.1063/1674-0068/31/cjcp1708181 